

Application of the Two-dimensional Numerical Simulation for the Description of Semiconductor Gas Sensors

D.Schipanski, Z.Gergintschew, J.Kositza

Technical University of Ilmenau, Institute for Solid State Electronics
PF 0565 Kirchoffstr.1, 98684 Ilmenau, Germany

Abstract

The implementation of models for the gas adsorption on metal-oxide-semiconductors in a two-dimensional device simulator is the subject of this paper. Further we give an application example for the simulation of the sensitive reactions and the electronic device in their exchange. For that we use a conductivity type gas sensor with a polycrystalline ZnO active layer.

1. Introduction

The usage of electronic devices like transistors and resistors is nowadays a common approach to realize the transducer function of modern chemical gas sensors. Moreover the development of gas sensors with a metal-oxide (like ZnO, SnO₂ or Ga₂O₃...) as sensitive layer is mainly empirical. That's why, it is useful to employ numerical simulation methods for the development, description and optimization of semiconductor gas sensors. For that it is necessary to use in addition to the equations for electrical behaviour description, models for the gas adsorption and for the corresponding electrical parameter modification of the sensitive layer and the device behaviour.

2. Model for the gas chemisorption and use in the simulator PROSA

The description of the adsorption effects is based on the 'electron theory of catalysis on semiconductors' by Wolkenstein [1], which has been used already by Geistlinger [2] for the description of gas sensitive effects. The main properties of this model are discussed in [2][3], so we will describe it here briefly by means of the oxygen adsorption on n-type metal-oxide-semiconductor. We consider the steady-state case with the following assumptions for temperatures under 700 K: adsorption without dissociation of the oxygen molecule and no reaction of the O-vacancies with the O₂ from the gas.



In [1] Wolkenstein considered the neutral 'weak' chemisorption as precursor of the charged 'strong' chemisorption. The first one acts as an acceptor state on the metal-oxide surface. The particle is strong chemisorbed after an electron exchange with the

metal-oxide and a surface charge arise due to the strong chemisorption.

As a result of the steady-state chemisorption consideration by Wolkenstein we have for the fractional surface coverage Θ with O_2^- the following isotherm, which describes the chemisorption in dependence on the semiconductor properties (E_f) of the sensitive surface

$$\Theta = \frac{N}{N_0} = \frac{\beta P_{O_2}}{\beta P_{O_2} + 1} \quad (2)$$

with

$$\beta = \frac{s_0}{\nu \sqrt{2\pi M k T} \exp\left(\frac{-Q^0}{kT}\right)} \frac{1}{f^0 \left[1 + \exp\left(\frac{E_f - E_c}{kT}\right)\right]} \quad (3)$$

where N is the density of occupied surface states; N_0 the density of the maximal available surface states; P_{O_2} the oxygen partial pressure; s_0 the adhesion coefficient; M the mass of the adsorbed particle; k the Boltzmann constant; T the lattice temperature; ν the phonon frequency of the adsorbed particle; Q^0 the weak chemisorption energy; E_c the energy of the conduction band edge; E_f the Fermi energy; f^0 , f the occupation probabilities for the weak or strong chemisorption.

The charging of the metal-oxide surface due to the strong chemisorption is given by the following expression:

$$Q'_{ad} = -eN_0\Theta^- = -eN_0f^-\Theta \quad (4)$$

with e as elementary electronic charge.

For the simulation of the complete sensor devices the Poisson equation (5), the equation for the adsorption charge (like Wolkenstein) (6) and the continuity equations for electron and holes (7)(8) have to be solved

$$\text{div}[Q'_{ad} - \epsilon \text{grad}\phi] = e(V_0^+ + 2V_0^{++} - n + p - N_A^- + N_D^+) \quad (5)$$

$$Q'_{ad} = -eN_0f^-\Theta(P_{O_2}, \phi \dots) \quad (6)$$

$$\text{div}J_n = eR \quad (7)$$

$$\text{div}J_p = -eR \quad (8)$$

where ϕ is the electrical potential; V_0^+ , V_0^{++} the density of the single and double ionized oxygen vacancies; N_A^- , N_D^+ the acceptor and donator doping density; n , p the electron and hole density; J_n , J_p the current density of electrons and holes.

The equation system (5)-(8) is solved self-consistently with the 2d device simulator PROSA [4], which was developed at the TU Ilmenau. PROSA uses the finite difference method.

3. Application on a semiconductor gas sensor

Up to now there are two types of semiconductor gas sensors. The first one uses the effect of the work function change on the metal-oxide sensitive layer surface due to the band bending caused by the adsorption charge. An example for such sensor device is the Suspended Gate Field Effect Transistor (SGFET). A detailed description of the SGFET and a modelling of the influence of such parameters like sensitive layer doping and thickness are presented in [3]. A second type of a semiconductor gas sensor is the conductivity one [5]. As shown in Fig.1 it consists of a insulating substrate, a polycrystalline metal-oxide semiconductor layer and two electrodes. The charging of

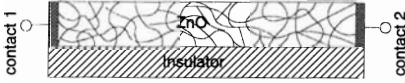


Figure 1: Schematic plot of a conductivity type gas sensor

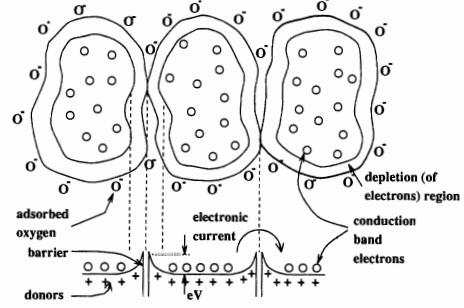


Figure 2: Mechanism of the conductivity change due to O_2 -chemorption

the grain surface due to the chemisorption has two effects on the layer conductivity. The first one is the influence of the potential barriers on the grain boundaries and the second one is the conductivity changing in the grain volumina due to the space charge regions (Fig.2).

For the simulation we divide the metal-oxide layer in several regions with regular shape, which represent the polycrystalline grains. We distinguish between compact sputtered metal-oxide sensitive layers, where the gas adsorption can take place only on the interface to the gas phase and the sintered metal-oxide layers, where the gas can diffuse around the grains. The schematic structures for the first case is shown in Fig.3. The current transport across the grain boundaries is considered to be controlled by the potential barrier, that means by the trap distribution or by the adsorption charge density at the boundaries. Effects like the thermionic emission (9) and recombination at the grain boundaries (10) are also taken into account.

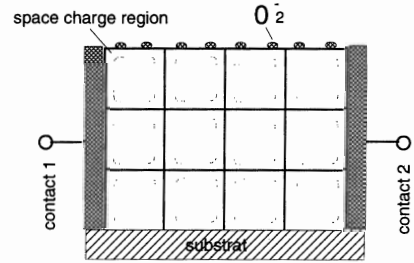


Figure 3: Schematic structure of the simulate conductivity type gas sensors with a compact metal-oxide layer

$$J = -\frac{A^*T^2}{N_C}(n_m - n_0) \quad \text{with} \quad n_0 = N_C \exp\left(-\frac{e\phi_B}{kT}\right) \quad (9)$$

$$R_s = \frac{np - n_i^2}{\frac{1}{s_p}(n + n_i) + \frac{1}{s_n}(p + n_i)} \quad (10)$$

Here are A^* the effective Richardson constant, ϕ_B the barrier height, n_m the electron density at nonequilibrium, n_i the intrinsic density and s the grain boundary recombination velocity.

In Fig.4 the current density distribution in a ZnO layer with 5×3 grains is shown for the case of gas adsorption only on the top-interface. The average grain size is 200nm, the O-vacancy density amount 10^{14} cm^{-3} and the applied voltage amount 2 Volt. The current flows always within the grains. It is smaller near at the surface and larger in the bulk of the ZnO layer. A cause for this current density distribution is on the one hand the depletion region at the ZnO-surface as a result of the oxygen chemisorption and on the other hand effect of the steady surface state density at the grain surface.

For the same case the relative resistance change by O_2 -adsorption is shown in Fig.5. One can see a nearly linear dependence between the relative resistance and the logarithm of oxygen partial pressure over a large region.

4. Summary

The chemisorption considered in dependence on the semiconductor properties of the sensitive surface and the compatibility with the equations of the drift-diffusion model are the main advantages of the adsorption description by Wolkenstein for our application. The first applications of the 2d-simulator PROSA show that it is a suitable tool for modelling of semiconductor gas sensors. PROSA offers the possibility to model the sensor devices completely that means the sensitive chemo-physical reactions and the transducer function of the electron devices in their exchange. For the application for sensors with other metal-oxide sensitive layers and different gases or gas mixtures one have to determine some of the needed input parameters.

Acknowledgement

This work has been supported by the German Federal Ministry for Research and Technology under Project Number 13 MV 0331 0. Further we acknowledge the support of Mr.H. Foerster and Mr.D. Nuernbergk with the basic version of the simulator PROSA.

References

- [1] T. Wolkenstein, "Electronic Processes on Semiconductor Surfaces during Chemisorption," *Consultants Bureau, New York*,1991.
- [2] H. Geistlinger, "Electron theory of thin-film gas sensors," *Sensors and Actuators B*, vol. 17, no. 1, pp. 47-60, 1993.
- [3] Z. Gergintschew, H. Foerster, J. Kositzka and D. Schipanski, "Two-dimensional numerical simulation of semiconductor gas sensors," *Sensors and Actuators B*, vol. 26, no. 1-3, pp. 170-173, 1995.
- [4] H. Foerster and D. Nuernbergk, "PROSA-3.0," Technische Universitaet Ilmenau, Institut fuer Festkoerperelektronik, 1995.
- [5] N. Tagutchi, "UK Patent specification 1280809," 1970.

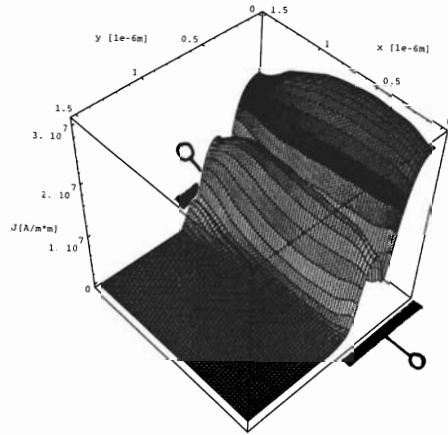


Figure 4: Current density distribution in a polycrystalline ZnO layer

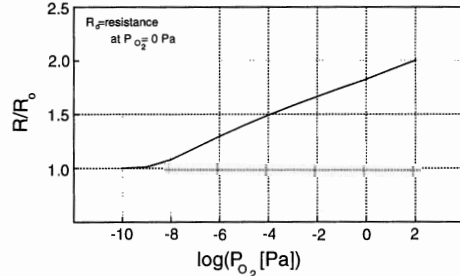


Figure 5: Relative resistance change of the ZnO layer by O_2 -adsorption

Analysis of Piezoresistive Effects in Silicon Structures Using Multidimensional Process and Device Simulation

M. Lades, J. Frank^a, J. Funk^b, G. Wachutka

Chair for Physics of Electrotechnology

Technical University Munich

Arcisstrasse 21, D-80290 Munich, GERMANY

^a Corporate Research and Development, Siemens AG

Otto-Hahn-Ring 6, D-81730 Munich, GERMANY

^b Physical Electronics Laboratory

Swiss Federal Institute of Technology

ETH-Hönggerberg, HPT, CH-8093 Zurich, SWITZERLAND

Abstract

With the view to analyzing piezoresistive effects in silicon microstructures we implemented a rigorous physically-based model in the multidimensional general purpose device simulator DESSIS^{ISE}. In this model, the dependence of the piezoresistive coefficients on temperature and doping concentration is included in a numerically tractable way. Using a commercial TCAD system (ISE), the practicability of the approach is demonstrated by performing a complete simulation sequence for realistic microdevices ranging from the layout design up to the analysis of the device operation.

1. Introduction

Mechanical distortion of silicon microstructures results in a change in the electric conductivity. In modern semiconductor technology this effect is employed in realizing smart integrated micromechanical sensors. On the other hand, piezoresistivity arises as undesired parasitic effect in silicon devices due to mechanical stress induced by thermal treatment or packaging. Up to now, a predictive numerical analysis of the performance of piezoresistive elements integrated in semiconductor microdevices was restricted to idealized structures with simplified geometry, assuming spatially uniform piezoresistive coefficients along high-symmetric crystal orientations without local dependence on the doping concentration or temperature distribution. Of course, with these quite coarse approximations a quantitative analysis of realistic devices is hardly possible. For accurate results a full multidimensional numerical simulation is required, which is based on a coupled field description of the piezoresistive effects. A reliable numerical approach is demonstrated in this work.

2. Modelling

A rigorous physically-based model [1] describing the strain-induced changes in the electric conductivity of single-crystalline silicon has been implemented in the multidimensional general purpose device simulator DESSIS^{ISE} [2]. The basic part of the model is a linear extension of the constitutive current relations for electrons and holes,

$$J_\alpha = -\sigma_\alpha \cdot (\bar{I} + \bar{\Pi}_\alpha \cdot \bar{X}) \cdot \bar{\nabla} \varphi_\alpha, \quad (\alpha = n, p)$$

where σ_α denotes the isotropic electric conductivity in the absence of stress, \bar{I} the identity tensor, \bar{X} the mechanical stress tensor, φ_α the quasi-Fermi potential and $\bar{\Pi}_\alpha$ the tensor of piezoresistive coefficients which depend on the doping concentration and the temperature distribution.

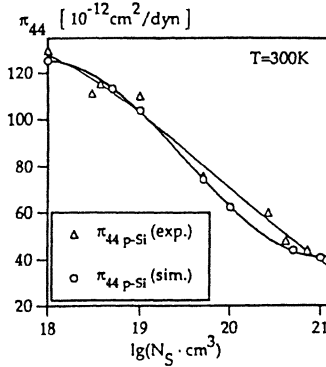


Fig. 1: Comparison of measured [3] and calculated piezoresistive shear coefficient Π_{44} in p-doped silicon versus concentration N_s of the diffused piezoresistive layer.

The implemented model was validated with reference to experimental piezoresistive coefficients measured in diffused n- and p-type silicon layers [3]. As shown in Fig. 1 for the shear coefficient Π_{44} in p-silicon, for instance, we achieved good agreement between simulation and measurement of the test structures.

3. Simulation of integrated silicon piezoresistive sensors

The capabilities of the interfaced simulation system were demonstrated by a complete simulation sequence ranging from layout and process simulation up to piezoresistive device simulation. Two realistic microtransducer structures fabricated by means of industrial silicon IC technology were investigated. Each of them is basically a square silicon diaphragm ($10 \times 1000 \times 1000 \mu\text{m}^3$) with integrated piezoresistors connected in a Wheatstone bridge. The first structure represents the conventional layout of a pressure sensor (Fig. 2) as proposed in [4]. The second device (Fig. 3) is an electrothermally excited microresonator with piezoresistive readout, which is used as test structure for determining thermoelastic material properties. The four piezoresistors of the Wheatstone bridge probe the thermoelastic deformations caused by a heating resistor placed at the diaphragm centre. Obviously the two structures are similar with respect to the mechanical behavior, but differ in the arrangement of the piezoresistors.

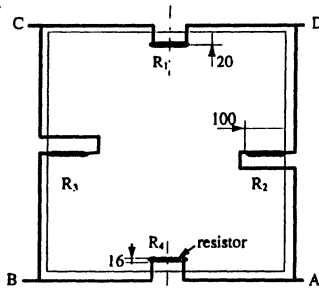


Fig. 2: Top view of a sensor structure for pressure measurement [4] (lengths in μm).

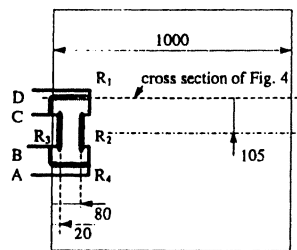


Fig. 3: Top view of a microresonator structure with piezoresistive readout (lengths in μm).

For easy comparison of the respective sensitivities, we assumed equal technological and geometrical parameters for both structures (namely those measured on the microresonator). The piezoresistors were fabricated using a boron implantation with subsequent drive-in diffusion. The maximum doping concentration amounts to $2 \times 10^{18} \text{ cm}^{-3}$ and is located at a depth of about $0.6 \mu\text{m}$. In our simulations we assumed that a pressure difference $\Delta p = p_1 - p_0$ between top and bottom side of the diaphragm caused the mechanical deformation (cf. Fig. 4).

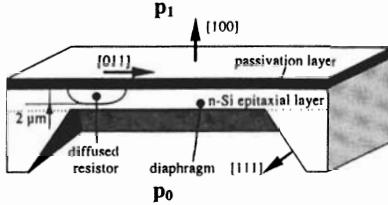


Fig. 4: Cross section of the simulated pressure sensor, showing crystal orientations and the location of the piezoresistors. p_0 is the reference pressure, p_1 the measurand.

The sequence of simulation steps is shown in Fig. 5. Using the two-dimensional technology simulator DIOS^{ISE} [5] all fabrication steps of the diaphragm and the piezoresistors can be simulated, yielding their doping profile.

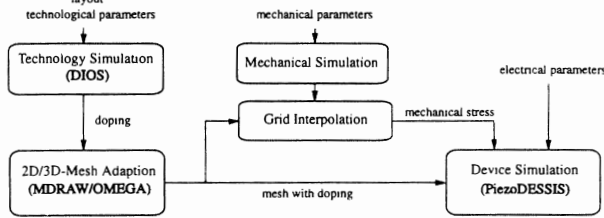


Fig. 5: Schematic simulation sequence and data flow.

The DIOS output mesh is adapted for the use in the piezoresistive simulation step by means of the automated grid manipulating programs MDRAW^{ISE} (2D) and OMEGA^{ISE} (3D). Multi-dimensional structural analysis is interfaced by projecting the resulting stress field onto the adapted grids. In order to achieve high accuracy in the calculation of the diaphragm deformation, the entire transducer structure (i.e., diaphragm and its suspension on bulk silicon) was taken into account. Also the passivation layer on top, consisting of $0.6 \mu\text{m}$ SiO_2 and $0.3 \mu\text{m}$ Si_3N_4 , was included in the simulation domain, since it is known that the mechanical behavior can significantly be influenced by that. Fig. 6 illustrates the different areas underlying the mechanical and the electrical simulations.

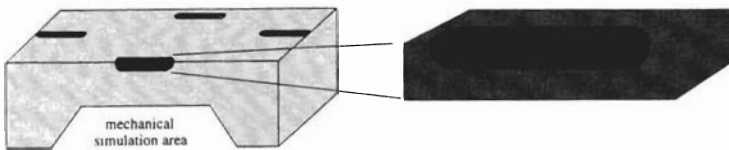


Fig. 6: Embedding of the electrical simulation domains in the full diaphragm structure used in the mechanical analysis.

Lastly, with the device structure and the field of mechanical stress as input, the extended DESSIS version computed the relative change in electrical resistivity $\Delta R_i / R_0$ ($i=1, \dots, 4$) for each of the piezoresistors. From this data, the output voltage of the Wheatstone bridge is determined according to [6]

$$V_{BD}/V_{AC} = \Delta V_{BD}/V_{AC} = (-\Delta R_1 + \Delta R_2 + \Delta R_3 - \Delta R_4) / R_0$$

where R_0 is the basic reference resistance and V_{AC} denotes the supply voltage. A reasonable measure of the pressure sensitivity S can be defined as

$$S = \Delta V_{BD} / (V_{AC} \cdot \Delta p)$$

Fig. 7 displays the calculated relative change of the bridge voltage versus the applied pressure difference. For the first example (pressure sensor), a sensitivity of $S = 6.1 \text{ mV} / (\text{V bar})$ was obtained. This value falls in a range typical of such an arrangement of piezoresistors, as it can easily be estimated from the functional dependence of the sensitivity on the diaphragm side length [6]. The sensitivity of the second structure (microresonator) was calculated to be $S = 1.1 \text{ mV} / (\text{V bar})$, which is significantly smaller than the measured value. Presumably the difference results from a calibration problem. In experiment, the deformation of the diaphragm was caused by the thermoelastic effect as mentioned above, and not by a uniform pressure difference as simulated. Reference for the calibration was the measured elongation at the diaphragm center which, of course, is not a linear measure of the overall deformation. A comprehensive simulation of the coupled thermo-mechanical effects inside the structure, planned as future work, should provide clarity.

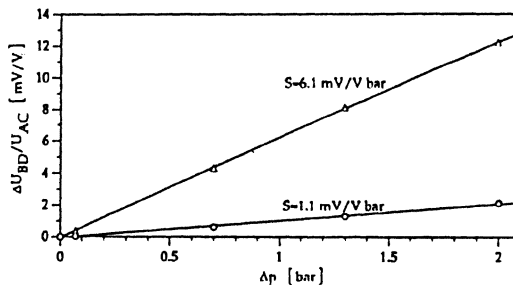


Fig. 7: Sensor response of the analyzed diaphragm structures (Δ structure from Fig. 2, o structure from Fig. 3).

4. Conclusion

The presented approach constitutes a practicable method for the numerical analysis of realistic piezoresistive structures. The practicability of a full simulation sequence ranging from layout and process simulation through structural analysis up to piezoresistive device simulation has been demonstrated with reference to realistic microtransducer structures.

5. Acknowledgement

The authors are grateful to U. Krumbain, Dr. N. Strecker and Dr. A. Schenk from the Institute of Integrated Systems, ETH Zurich, for providing helpful assistance and technical support.

References

- [1] Z. Z. Wang, "Modélisation de la Piézoresistivité du Silicium", *PhD thesis* No. 9929, Univ. of Science and Technology, Lille, France (1994).
- [2] DESSIS^{ISE} Reference Manual Version 1.3 (1994), Institute of Integrated Systems, ETH Zurich (1993).
- [3] O. N. Tufté, E. L. Stelzer, "Piezoresistive Properties of Silicon Diffused Layers", *J. Appl. Phys.* **34** (1963) 313-318.
- [4] K.W. Lee, K. D. Wise, "SENSIM: A Simulation Program for Solid-State Pressure Sensors", *IEEE Trans. on ED*, vol. **ED-29** (1982) 34.
- [5] N. Strecker, DIOS^{ISE} User's Manual, Institute of Integrated Systems, ETH Zurich (1993).
- [6] P. Ciampolini et al, "Electro-Elastic Simulation of Piezoresistive Pressure Sensors", in *Simulation of Semiconductor Devices and Processes*, vol. 5, ed. by S. Selberherr et al, Springer, Vienna (1993) 381-384.